

## PREPARATION OF SYNTHESIS NANOPARTICLES $Fe_3O_4$ BASED ON IRON SAND SUMBAWA

Syamsul Bahtiar<sup>1\*</sup>, Fauzi Widyawati<sup>1</sup>, Emsal Yanuar<sup>1</sup>, Risky Ramadhan<sup>1</sup>, Karen Zahra<sup>1</sup>, and Syamsul Hidayat<sup>2</sup>

<sup>1</sup>Department of Metallurgical Engineering, Faculty of Mineralogy and Environmental Technology. Sumbawa University of Technology, Sumbawa, Indonesia.

<sup>2</sup>Department of Environmental Engineering, Faculty of Mineralogy and Environmental Technology. Sumbawa University of Technology, Sumbawa, Indonesia.

\*Email: [syamsul.bahtiar@uts.ac.id](mailto:syamsul.bahtiar@uts.ac.id)

Received: September 8, 2023. Accepted: : November 7, 2023. Published: November 30, 2023

**Abstract:** Iron sand generally contains minerals such as ilmenite, magnetite, and hematite. Based on the results of previous tests, the main composition of iron sand in Rhee, Sumbawa regency, is magnetite. One method to increase the Fe content in iron sand is by pre-treatment with NaOH. NaOH is also used to precipitate heavy metals in a mineral. In this study, three variations were carried out with the ratio of NaOH: iron sand, namely: 1: 4, 2: 4, and 3: 4 at a temperature of 300 C. Furthermore, the calcination results were followed by the synthesis of  $Fe_3O_4$  nanoparticles using the coprecipitation method. The results of the XRF characterization showed an increase in Fe levels after being processed by the alkalization treatment. The highest concentration was obtained in 1:4, with a Fe percentage of 91.1%. The results of the XRD characterization showed that the synthesis of  $Fe_3O_4$  was successfully carried out with single phase  $Fe_3O_4$  according to the data reference 96-9005839 forms and the space group F d -3 m. Crystal size analysis Using the Debey-Scherrer equation, the respective sizes were 12.7 nm, 8.71 nm, and 9.76 nm, respectively.

**Keywords:** Iron Sand, Alkalization, XRF, XRD, Nanoparticles, Magnetite

### INTRODUCTION

One of the abundant natural resources in Indonesia is iron sand, which can be found on a beach north of Sumbawa, West Nusa Tenggara. Generally, iron sand contains some valuable minerals, including the mineral ilmenite  $FeTiO_3$ , magnetite ( $Fe_3O_4$ ), and hematite ( $Fe_2O_3$ ) [1]. However, each area containing iron sand has its content and composition, such as the Banten area, primarily composed of *ilmenite* minerals. Meanwhile, Lumajang, Tulungagung, and Sumbawa NTB mainly comprise magnetite minerals.

Nowadays, extensive study is being carried out on  $Fe_3O_4$  nanoparticles because  $Fe_3O_4$  has unique properties like superparamagnetic in nanosize. This nature has developed into fundamentals that can be applied in a variety of fields, such as drug delivery system agents (DDS) [2], radar absorption [3], supercapacitors [4], photocatalytic [4], and magnetic sensors [5,6].

Several methods for producing  $Fe_3O_4$  nanoparticles exist, including sol-gel [7], hydrothermal [8], coprecipitation [9], and sonochemistry [10,11]. The coprecipitation method is one effective method of producing  $Fe_3O_4$  nanoparticles. Besides being quickly done, it can be carried out in an atmosphere with controlled temperatures [12]. Using the coprecipitation approach, we could generate nanoparticles with particle sizes ranging from 3 to 20 nm from ferrous and ferric salts in a hydroxide medium under various conditions [13].

Consider that a broad application requires synthesis to obtain the purity phase. The attempt purification can be accomplished using a method known as alkaline treatment with NaOH. NaOH can

precipitate heavy metals and control water acidity [13, 14]. In the previous study of  $TiO_2$  extraction from iron sand, Banten used the method of fusion caustic, which consists of reacting iron sand with targeted NaOH to break the bond Fe-Ti-O compound in ilmenite and form frits [15]. Furthermore, purified iron using an alkalization method. The results showed that the impurities of the elements Si, P, and Al were successfully eliminated at a NaOH concentration of 5M and a sintering temperature of 250C. The higher the NaOH concentration utilized, the higher the iron production rate [16].

Based on the description above, this will be done in research with enhancement rate iron on iron sand with method alkalization. This will define the use of XRF to determine the percentage composition of iron due to alkalization. The XRD characterization then seeks to determine the system crystal, purity phase, and crystal size. X-rays from the diffraction method can describe grid parameters, structure types, the arrangement of different atoms in the crystal, crystal imperfections, orientation, grains, and size items [17].

### RESEARCH METHODS

#### Materials

The materials used in this research were iron sand from Sumbawa, sodium hydroxide (NaOH), ammonium hydroxide ( $NH_4OH$ ), and distilled water.

#### Sample Preparation

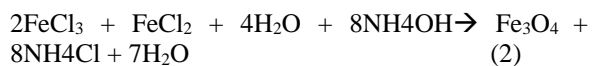
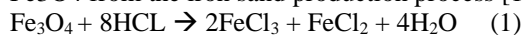
The procedure begins with separating iron sand from soil using permanent magnets. Prepare 20 grams of iron sand and 5, 10, and 15 grams of NaOH

for alkalization. The alkalization process is carried out by mixing NaOH with iron sand, called the caustic fusion process. The cutting fusion process is carried out to break down impurity minerals in iron sand. This process was carried out at a temperature of 300C for 60 minutes.

Furthermore, water leaching is carried out for 30 minutes at temperatures 75C to decompose NaOH from iron sand. In the final step, the iron sand is filtered and dried. Use the oven for 1 hour at a temperature of 100C.

**Synthesis of Fe3O4 nanoparticles**

The coprecipitation approach was used to synthesize Fe3O4 nanoparticles in HCL solvent. At room temperature, 20 grams of iron sand reacted with 60 ml HCL on a magnetic stirrer for 30 minutes. During the process, the NH4OH solution was continually lowered until a precipitate of Fe3O4 nanoparticles formed. The residue is then rinsed with distilled water until the pH is neutral. Furthermore, the Fe3O4 residue was dried at 100°C for 1 hour. The following equation describes the reaction of the Fe3O4 from the iron sand production process [18]:



**Material Characterization**

The X-ray fluorescence (XRF) technique is used to analyze the element composition on iron sand, and the X-ray diffraction (XRD) technique is used to study crystal size, phase, structure, and grid parameters—PANalytical Type X’Pert Pro XRD characterization).

**RESULTS AND DISCUSSION**

**XRF (X-Ray Fluorescence) Analysis**

XRF characterization was carried out to determine the composition and levels of elements contained in iron sand before and after NaOH treatment. This identification technique is based on X-ray counting, which occurs due to photoelectricity. Based on the characterization results of each variation, as shown in Table 1.

Table 4.1 shows the XRF characterization results of iron sand samples with alkalization and without alkalization. The result indicates that the composition of the Fe element in the model was as big as 82.60% at the beginning. Meanwhile, the composition element Fe with alkalization experiences increasing and successfully as big as 91.1%, 90.62%, and 90.55%. Based on the characterization of the results, the use of optimal alkalization in research is variation 1:4. The Ca, Ti, and P elements have been successfully reduced in composition. Based on Table 4.1, it can also be seen that results alkalization can reduce rate impurities in iron sand; even Al, Si, and K content of around 5.6% was successfully removed in a

way overall on each variation alkalization. With loss impurity in a way, direct Fe levels will increase. Ascension marks Fe content of sample beginning to sample with variation acquisition highest own range of 8.50%. Based on the results, we can conclude that alkalization effectively increases iron composition in iron sand. Content iron Rhee Beach Sumbawa is classified as tall, which is as big as 82.60%, different from the rate iron sand found in the Tulungagung area content iron (Fe) by 86% [1].

Table . XRF characterization of iron sand treatment outcomes alkalization

Element	Without Treatment	Composition (%)		
		1:4	2:4	3:4
P	0.46	0.2	0.2	0.2
Ca	1.74	0.66	1.08	1.14
Ti	6.09	4.46	4.78	4.88
V	0.54	0.47	0.33	0.28
Cr	0.099	0.099	0.11	0.098
Mn	0.67	0.78	0.72	0.71
Fe	82,60	91.10	90.62	90.55
Zn	0.08	0.06	0.07	0.05
Rb	0.38	0.57	0.50	0.54
Eu	0.57	0.63	0.64	0.63
Re	0.3	0.3	0.20	0.2
Ms	0.76	0.74	0.76	0.73
Al	3	-	-	-
Si	2.6	-	-	-
K	0.13	-	-	-
Other	0.26	-	-	-

**XRD (X-Ray Fluorescence) Analysis**

**Analysis of crystal structure**

The phase, size Kristal, structure crystal, and lattice characteristics of Fe3O4 nanoparticles were determined by XRD characterization. The XRD analysis findings are processed using the X’pert application Highscore Plus to acquire data about the structural crystal. The data is validated using Crystallography Open Database (COD) as the grid database reference crystal. The XRD test results were charted using pattern diffraction, as shown in Figure 1.

Figure 1 Represents the results of the XRD characterization of samples of Fe3O4 nanoparticles. The XRD data indicate polycrystalline in a qualitative study. Peak diffraction from a piece discovered in 2θ: 30.16 0, 35.52 0, 43.17 0, 57.11 0, and 62.71 0, each with mark field crystals (220), (311), (222), (400), (422), and (511). Based on the corners created and the matching with the field crystal, we may look for a new peak so the resultant magnetite has a high purity. This result is also supported by previous XRF testing with Fe content above 90%. Besides that, Fe levels also affect the intensity of the resulting diffraction. The sample with

variation 1; 4 shows more tall peaks than the two models. High intensity shows that the crystal has its regularity. Good crystal or degrees the crystal higher and higher, and many atoms are arranged orderly and neatly. Quantitative analysis may be performed with several XRD findings approaches, including using various software, one of which is HSP. HSP analysis with code reference 96-9005839 reveals a pattern of diffraction magnetite that is a 100% match. Based on the data, magnetite has a crystal system Cubic and a shaping room group Fd-3m [19]. The cubic spinel structure Fe<sub>3</sub>O<sub>4</sub> can be illustrated in Figure 2.

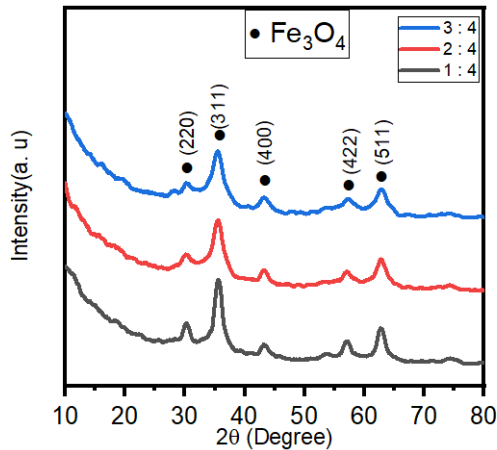


Figure 1. Diffraction pattern Fe<sub>3</sub>O<sub>4</sub> Nanoparticles.

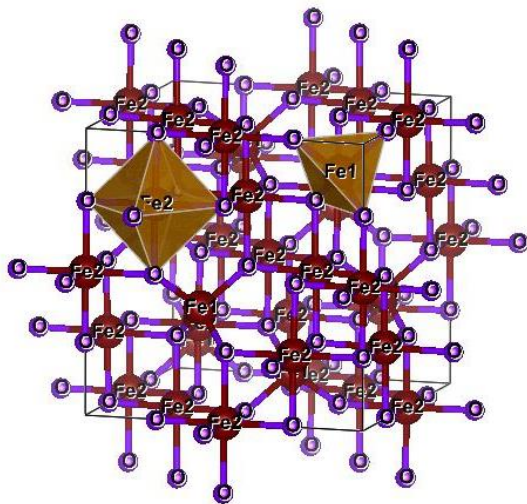


Figure 2. Cubic structure of magnetite nanoparticles. The mineral Fe<sub>3</sub>O<sub>4</sub> cubic spinel system atoms are arranged as Fe<sup>2+</sup>, Fe<sup>3+</sup>, and oxygen. In a sense, Fe<sup>2+</sup> and Fe<sup>3+</sup> will bind oxygen in the tetrahedral and octahedral regions. [20].

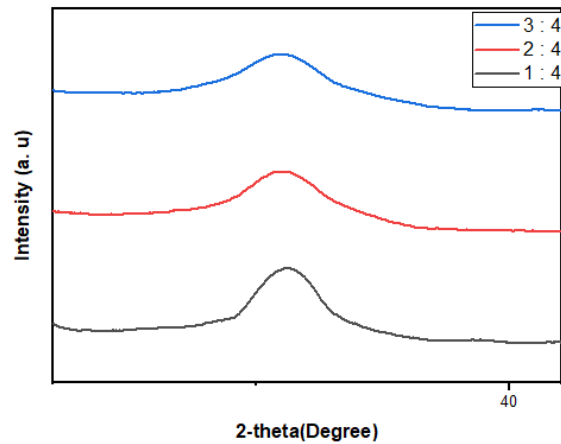
### Crystal Size Analysis

The analysis of the size of the deck crystal is done using the Debye-Scherrer equation [21]:

$$D = \frac{K\lambda}{\beta \cos\theta} \quad (3)$$

D represents the crystal size, K is a constate (0.9), β is the width at half maximum, and θ is the diffraction angle.

The FWHM value at the highest peak can be used to calculate crystal size. The prominent peak is created at a blade angle of 35 degrees based on the diffraction pattern of Fe<sub>3</sub>O<sub>4</sub> nanoparticles. The results are shown in Figure 3.



Gambar 3: Fitting FWHM pada puncak utama nanoparticle Fe<sub>3</sub>O<sub>4</sub>

Based on Figure 3, the analysis qualitatively showed a higher diffraction peak and a smaller peak width in sample 1:4. In contrast, the peak height decreased for samples 2:4 and 3:4, and the peak width grew. The higher the peaks and the smaller the peaks were displaced, the smaller the crystal size. The result of the calculation of the crystal size using the debye-Scheerer equation was the size of 12.7nm, 8.71 nm, and 9.76 nm.

### CONCLUSION

Studies on the impact of alkalization on iron sand rate and the production of magnetite nanoparticles based on iron sand have been successful. Test results rate beginning sand Rhee iron is obtained amounting to 82.60%. Meanwhile, the characterization test results rate with treatment alkalization received consecutive as big as 91.10% (1:4), 90.62% (2:4), and 90.55% (3:4). Synthesis magnetite nanoparticles have also succeeded with method coprecipitation. Quantitative analysis was performed using high score Plus (HSP), and data successfully confirmed matching with reference code 96-9005839. Based on the matching results, single-phase magnetite is obtained. Meanwhile, the crystal size calculations were 12.7nm, 8.71 nm, and 9.76 nm.

### ACKNOWLEDGEMENTS

The authors thank KEMENDIKBUDRISTEK RI for providing a research grant via the “PDP Scheme” for SBAHTIAR in 2023.

### REFERENCES

- [1] Ajeng Hefdea & Lydia Rohmawati. (2020a). Sintesis Fe<sub>3</sub>O<sub>4</sub> dari Pasir Mineral Tulungagung Menggunakan Metode Kopresipitasi. *Jurnal Inovasi Fisika Indonesia*.

- [2] Li, X., Lv, W., Yang, W., Guo, Y., Huang, J., Liang, W., Huang, Y., Qin, A., Deng, X., Li, X., Chen, M., Yang, H., Liang, L., & Du, L. (2023). Poly (hydroxyethyl methacrylate—Acrylic acid) microspheres loaded with magnetically responsive Fe<sub>3</sub>O<sub>4</sub> nanoparticles for arterial embolization, drug loading, and MRI detection. *Journal of Drug Delivery Science and Technology*, 79, 103993.
- [3] Ahmad Taufiq, S. Bahtiar, Sunaryono, Nurul Hidayat, A. Fuad, M. Diantoro, Arif Hidayat, Suminar Pratapa, & Darminto. (2010). Kajian Struktur Kristal Dan Dielektrisitas Nanopartikel Magnetite Berbasis Pasir Besi Doping Zn<sup>2+</sup> Hasil Sintesis Metode kopresipitas. *Jurnal Sains Materi Indonesia*.
- [4] Gross, M. A., Monroe, K. A., Hawkins, S., Quirino, R. L., Moreira, S. G. C., Pereira-da-Silva, M. A., De Almeida, S. V., Faria, R. C., & Paterno, L. G. (2022). High-performance supercapacitor electrode based on a layer-by-layer assembled maghemite/magnetite/reduced graphene oxide nanocomposite film. *Journal of Electroanalytical Chemistry*, 908, 116123.
- [5] Ariti, A. M., Geleto, S. A., Gutema, B. T., Mekonnen, E. G., Workie, Y. A., Abda, E. M., & Mekonnen, M. L. (2023). Magnetite chitosan hydrogel enzyme with intrinsic peroxidase activity for smartphone-assisted colorimetric sensing of thiabendazole. *Sensing and Bio-Sensing Research*, 42, 100595.
- [6] Maroju, P. A., Ganesan, R., & Dutta, J. R. (2022). Fluorescence-based simultaneous dual oligo sensing of HCV genotypes 1 and 3 using magnetite nanoparticles. *Journal of Photochemistry and Photobiology B: Biology*, 232, 112463.
- [7] Lemine, O. M., Omri, K., Zhang, B., El Mir, L., Sajjeddine, M., Alyamani, A., & Bououdina, M. (2012). Sol-gel synthesis of 8nm magnetite (Fe<sub>3</sub>O<sub>4</sub>) nanoparticles and their magnetic properties. *Superlattices and Microstructures*, 52(4), 793–799.
- [8] Molina-Calderón, L., Basualto-Flores, C., Paredes-García, V., & Venegas-Yazigi, D. (2022). Advances of magnetic nano hydrometallurgy using superparamagnetic nanomaterials as rare earth ions adsorbents: A grand opportunity for sustainable rare earth recovery. *Separation and Purification Technology*, 299, 121708.
- [9] Nkurikiyimfura, I., Wang, Y., Safari, B., & Nshingabigwi, E. (2020). Temperature-dependent magnetic properties of magnetite nanoparticles synthesized via coprecipitation method. *Journal of Alloys and Compounds*, 846, 156344.
- [10] Prasetyowati, R., Widiawati, D., Swastika, P. E., Ariswan, A., & Warsono, W. (2021). Sintesis dan Karakterisasi Nanopartikel Magnetit (Fe<sub>3</sub>O<sub>4</sub>) Berbasis Pasir Besi Pantai Glagah Kulon Progo dengan Metode Kopresipitasi pada Berbagai Variasi Konsentrasi NH<sub>4</sub>OH. *Jurnal Sains Dasar*, 10(2), 57–61.
- [11] Rahmawati, R., Taufiq, A., Sunaryono, S., Fuad, A., Yulianto, B., Suytman, S., & Kurniadi, D. (2018). Synthesis of Magnetite (Fe<sub>3</sub>O<sub>4</sub>) Nanoparticles from Iron Sands by Co—Precipitation—Ultrasonic Irradiation Methods. *Journal of Materials and Environmental Sciences*, 9(1), 155–160.
- [12] Sunaryono, Taufiq, A., Mashuri, Pratapa, S., Zainuri, M., Triwikantoro, & Darminto. (2015). Various Magnetic Properties of Magnetite Nanoparticles Synthesized from Iron-Sands by Coprecipitation Method at Room Temperature. *Materials Science Forum*, 827, 229–234.
- [13] Glory Riama, Austrin veranika, & Prasetyowati. (2012). The Effect of H<sub>2</sub>O<sub>2</sub>, NaOH Concentration and Time on the Degree of White Pulp From Pineapple Crown. *Jurnal Teknik Kimia*, 18, No.3.
- [14] Hidayat, S., Desiasni, R., & Novia, N. (2023). Effect of addition of an organic inhibitor of kersen leaf extract (*Muntingia calabura* L) on corrosion rate on A36 steel in seawater media. *Jurnal Pijar Mipa*, 18(4), 601–607.
- [15] Aristanti, Y., Supriyatna, Y. I., Masduki, N. P., & Soepriyanto, S. (2018). Decomposition of banten ilmenite by caustic fusion process for TiO<sub>2</sub> photocatalytic applications. *IOP Conference Series: Materials Science and Engineering*, 285, 012005.
- [16] Su, B., Mochizuki, Y., Higuchi, K., & Tsubouchi, N. (2023). Effects of various factors on gangue removal in alkaline hydrothermal treatment of iron ores. *Minerals Engineering*, 203, 108329.
- [17] Bahtiar, S., Taufiq, A., Sunaryono, Hidayat, A., Hidayat, N., Diantoro, M., Mufti, N., & Mujamilah. (2017). Synthesis, Investigation on Structural and Magnetic Behaviors of Spinel M-Ferrite [M = Fe; Zn; Mn] Nanoparticles from Iron Sand. *IOP Conference Series: Materials Science and Engineering*, 202, 012052.
- [18] Taufiq, A., Bahtiar, S., Saputro, R. E., Yuliantika, D., Hidayat, A., Sunaryono, S., Hidayat, N., Samian, S., & Soontaranon, S. (2020). Fabrication of Mn<sub>1</sub>Zn Fe<sub>2</sub>O<sub>4</sub> ferrofluids from natural sand for magnetic sensors and radar-absorbing materials. *Heliyon*, 6(7), e04577.
- [19] Radoń, A., Kubacki, J., Kądziołka-Gaweł, M., Gębara, P., Hawełek, Ł., Topolska, S., & Łukowiec, D. (2020). Structure and magnetic properties of ultrafine superparamagnetic Sn-doped magnetite nanoparticles synthesized by glycol-assisted coprecipitation method. *Journal of Physics and Chemistry of Solids*, 145, 109530.

- [20] Taufiq, A., Saputro, R. E., Susanto, H., Hidayat, N., Sunaryono, S., Amrillah, T., Wijaya, H. W., Mufti, N., & Simanjuntak, F. M. (2020). Synthesis of Fe<sub>3</sub>O<sub>4</sub>/Ag nanohybrid ferrofluids and their applications as antimicrobial and antifibrotic agents. *Heliyon*, 6(12), e05813.
- [21] Arif, S., Nawaz, M., Siddique, S., Ayub, R., & Saleem, S. (2022). Synthesis, characterization, and photocatalytic activity of Mg<sub>1-x</sub>Cu<sub>x</sub>O nanoparticles for wastewater treatment. *Materials Today Communications*, 33, 104361.